Macromolecules

Volume 23, Number 14 July 9, 1990

Development of Crystallinity in a Polyurethane Containing Mesogenic Units. 1. Morphology and Mechanism

G. Smyth,[1a] E. M. Vallés,[1b] S. K. Pollack,[1c] J. Grebowicz,[1d] P. J. Stenhouse, S. L. Hsu,* and W. J. MacKnight*

Department of Polymer Science and Engineering, University of Massachusetts, Amherst, Massachusetts 01003

Received May 2, 1989; Revised Manuscript Received December 14, 1989

ABSTRACT: This work extends prior studies of a polyurethane containing mesogenic moieties. Optical and thermal methods reveal that this polyurethane exhibits monotropic mesomorphic behavior. Two distinct crystallization mechanisms and crystal morphologies are identified, one arising from the isotropic melt and producing a spherulitic texture and the other arising from the mesophase and producing a threaded texture. A combination of thermal analysis, X-ray diffraction, and dynamic rheological studies reveals that crystals grown from the mesophase are readily perfected to a higher melting form by annealing whereas spherulitic crystals are less amenable to perfection. The development and perfection of the crystalline state were also found to be dependent on polyurethane molecular weight.

Introduction

Recently, there has been a considerable body of work detailing the process of crystallization and the nature of the crystalline phase in thermotropic liquid crystalline polymers.[2-12] The crystalline phase exhibited by these polymers is unusual, as the majority of the materials studied are either random copolymers or polymers composed of monomers which have substituents capable of random substitution along the chain. Major interest in materials of this type has focused on the liquid crystalline state which these polymers exhibit. While the special melt rheological properties of the liquid crystal state hold great promise for enhanced processing and the potential for generating self-reinforcing structures, it is the crystalline phase which determines their ultimate solid-state properties.

Recently, Wendorff and co-workers have observed that in a number of rigid rod thermotropic polyesters annealing at high temperatures causes the development of a high melting crystalline phase.[7] On the basis of the observed low entropy and enthalpy of fusion, as well as X-ray diffraction data, these workers propose that in these polymers the crystalline state is disordered.[3] From an Avrami analysis of crystallization kinetics, it was inferred that the crystallization process is complex, consisting of a fast process which involves ordering of the nematic melt and a slow process involving the development of a three-dimensional ordering between the chains. Windle and Blackwell and co-workers have also addressed the nature of the crystalline state in such materials through their investigations of rigid random copolyesters and have postulated a form of three-dimensional crystalline order which derives from the nematic phase of these polymers.[8-12] Previous studies of poly(4,4′-bis(6-hydroxyhexoxy)biphenyl-2,4-toluenediisocyanate) (24TDI/BHHBP) focused on aspects of the liquid crystalline state in this material.[13,14] The asymmetric position of the methyl group in the 2,4-toluenediisocyanate monomer causes it to be randomly substituted along the polymer chain. Despite this type of disorder, it was observed that these polyurethanes were in fact semicrystalline.

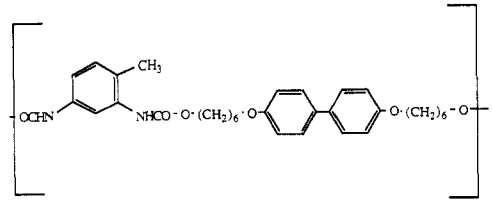

This paper presents the results of detailed investigations into the temperature-dependent phase behavior of these polyurethanes and resolves much of the observational/interpretational discrepancies touched upon in the earlier papers.[15] More importantly, in the present paper attention is focused upon the complex crystallization processes occurring in these polymers, which are found to be similar to those observed in other thermotropic polymers. An attempt is made to rationalize the thermal

0024-9297/90/2223-3389$02.50/0

behavior of these polyurethanes in terms of existing models for the crystallization of liquid crystalline polymers and to relate these observations to the growing body of literature pertaining to the development of crystallinity in these polymers. The formation of different macroscopic crystal morphologies is discussed, and some speculation as to the presence of mesogenic moieties inducing crystallizability is given. In subsequent publications, the nature of the microstructure and dynamics of the crystalline phase of 24TDI/BHHBP will be addressed.

Experimental Section

Materials. The synthesis of 24TDI/BHHBP has been described elsewhere.[13] The polymer referred to as low molecular weight was determined to have an intrinsic viscosity of 0.46, and the polymer referred to as high molecular weight had an intrinsic viscosity of 0.60, both measured in dimethylformamide.

Optical Microscopy. Optical microscopy was performed on a Carl Zeiss Ultraphoto II polarizing microscope equipped with a Linkham Scientific Instruments TMS 90 temperature controller and a TMH 600 hot stage. The hot stage temperature was calibrated with vanillin and potassium nitrate melting point standards.

Thermal Analysis. DSC measurements were performed on a Perkin-Elmer DSC 7 employing a 20 mL/min flow of dry nitrogen as purge gas for the sample and reference cells and an ice–water bath as coolant. The temperature and power ordinates of the DSC were calibrated with respect to the known melting point and heat of fusion of a high-purity indium standard. For exothermic and endothermic processes the peak temperatures were taken as the transition temperatures, while for the glass transition the midpoint of the heat capacity step was taken as the transition temperature.

Samples which were annealed for long times at high temperatures were scanned again in the DSC after melting so as to ensure that thermal degradation had not affected their thermal behavior. Provided the annealing was performed under nitrogen gas or vacuum, there were no observable changes in behavior.

Dynamic Rheology. Polymer samples were vacuum molded into disks (d = 25 mm, h = 2 mm) for the rheological measurements. These were performed on a Rheometrics dynamic spectrometer (RDS) in the parallel plate mode. After the desired thermal history was applied to each sample, it was annealed in the rheometer at 174 °C for 2.5 h. The storage and loss moduli, G' and G'', were measured at constant frequency (1 rad/s) during the annealing process. Nitrogen was continuously circulated in the environmental chamber of the instrument to minimize sample degradation. When the annealing process was completed, the samples were cooled in the rheometer and small pieces were separated from the disks for X-ray and DSC analysis.

X-ray Diffraction. X-ray diffraction data were obtained by using monochromatic Cu Kα radiation and a Nicolet Xentronics two-dimensional position-sensitive detector and data system. Data were collected for 20 min, and background scans of equivalent duration were subtracted to remove background scatter. The two-dimensional data were then azimuthally averaged to generate 2θ versus intensity scans.

Results and Discussion

The initial findings of crystallinity in 24TDI/BHHBP were based on the observation of narrow reflections in X-ray scattering studies. However, as was alluded to in the Introduction, some discrepancies were apparent in the interpretation of the phase behavior put forward in the earlier studies.[13] In order to better understand the temperature-phase behavior of these polymers and to provide a basis for the interpretation of other results, the optical textures obtained by cooling samples of high and low molecular weight polyurethane from the melt to a variety of annealing temperatures were studied by polarized light microscopy. The results are shown in Figure 1. Samples annealed at 150 and 140 °C give banded spherulitic textures with a negative birefringence as determined by the insertion of a first-order red plate into the optical path of the microscope.[16,17] Upon heating, it was observed that the spherulitic textures disappeared in the temperature range 165–170 °C.

The textures observed for samples annealed at 130 °C are less distinct in the photographs but, to the eye, appear threaded in character. When cooled to 130 °C, this type of texture develops quite rapidly. Slight shearing and heating of the sample to approximately 135 °C enhance more clearly the threaded textures (Figure 2), which are akin to those reported for a variety of liquid crystalline polymers.[18,19] It was observed that in the first few minutes after these threaded textures formed the sample could be sheared with relative ease and that the texture appeared and disappeared reversibly over a small temperature interval between 130 and 140 °C. Annealing for longer times or further cooling below 130 °C did not result in any change in the appearance of these samples. However, it was observed that the samples solidified and fractured. Once solidified, the threaded texture remained unchanged upon reheating up to temperatures in the range 165–170 °C, where it eventually disappeared. This suggests that crystallization from the mesophase occurs. It is noteworthy that in samples annealed above 140 °C and then cooled to lower temperatures (to produce mixed threaded and spherulitic textures) the spherulitic textures persisted to slightly higher temperatures than the solidified threaded background upon reheating, indicating a slightly higher melting point for the spherulitic crystals.

The observation of a fluid mesophase indicates the existence of a liquid crystalline phase in these polyurethanes when cooled rapidly from the melt. However, this phase is unstable and crystallizes spontaneously on annealing or on further cooling to produce a crystal phase with a higher melting point than the isotropization temperature of the mesophase. The mesophase is thus monotropic.[20,21] The macroscopic structures formed upon rapid cooling are poorly organized and reflect the initial threaded texture of the mesophase. The crystalline spherulites, which exhibit a slightly higher melting point, have a more regular macroscopic organization—probably due to the higher mobility available at the higher annealing temperatures.

Having established the basic phase–temperature behavior of these materials, we employed differential scanning calorimetry to provide more detailed information about the phase transitions and the effects of thermal history. It is noteworthy that, since these materials are monotropic, it is possible to grow crystals from either the isotropic melt or from the mesophase. With the ability to produce the two macroscopic morphologies independently, their individual thermal characteristics can be determined.

Typical heating and cooling traces recorded at 10 °C/min for a low molecular weight polyurethane are illustrated in Figure 3. Upon heating, the glass transition is observed at approximately 85 °C. This is followed by a region of exothermic behavior, typical of "cold crystallization", peaking at about 110 °C but continuing until the onset of melting as characterized by the two endothermic peaks at 158 and 170 °C. Since the polymer is identified as being monotropic, these two endothermic peaks must both be associated with crystal melting and not with the crystal–mesophse and mesophase–isotropic transitions, respectively.

After the melt is cooled, two exotherms at approxi-

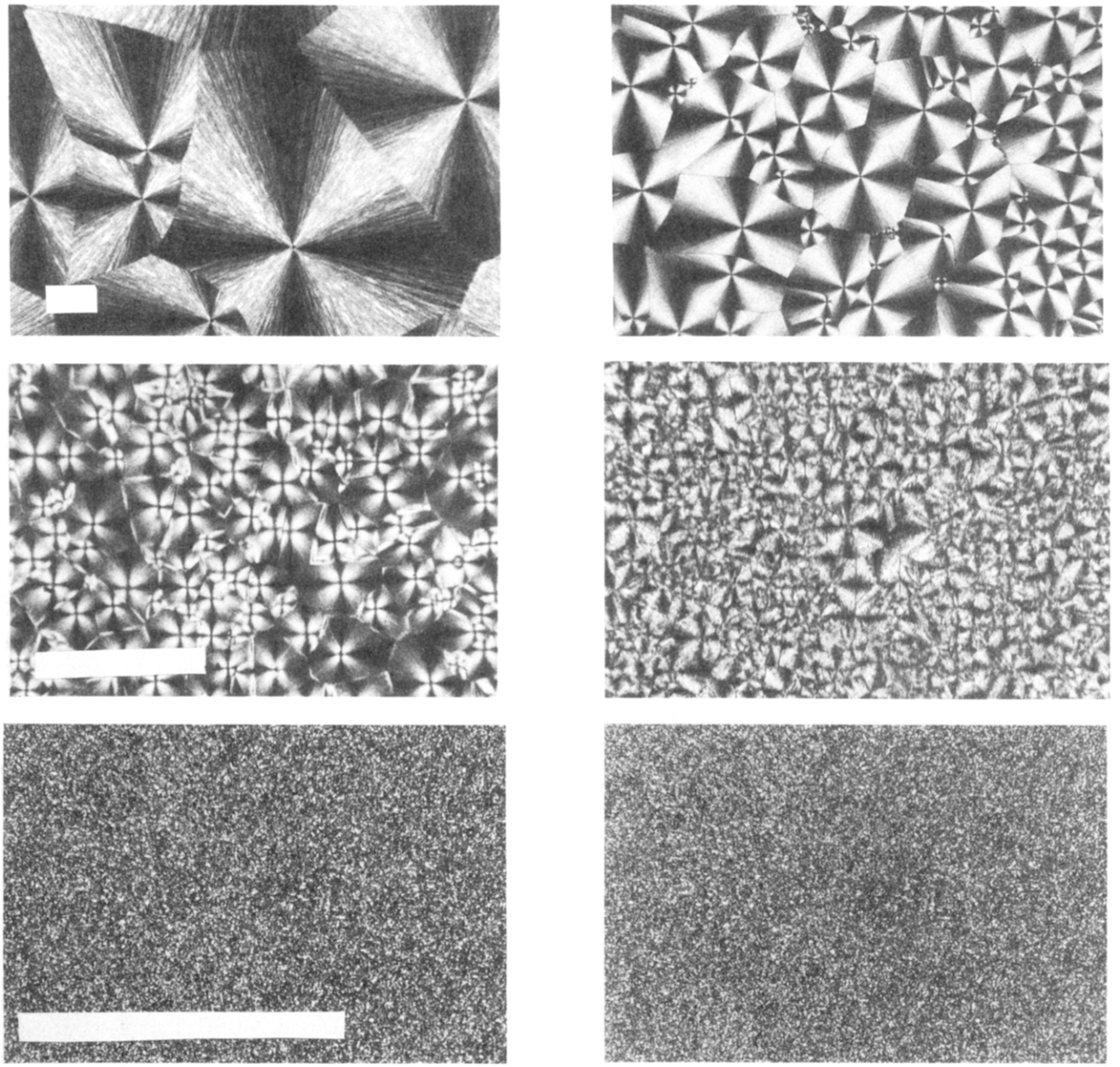

Figure 1. Various optical micrographs of 2-4TDIBHHBP showing spherulitic and threaded textures. Bar represents 100-μm marker.

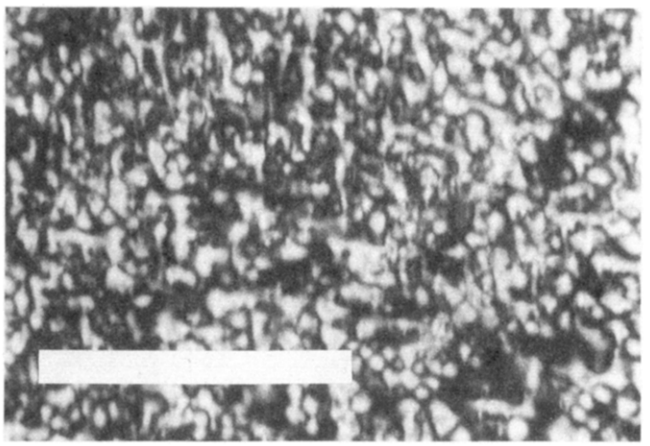

Figure 2. Threaded texture optical micrographs. Bar represents 100-μm marker.

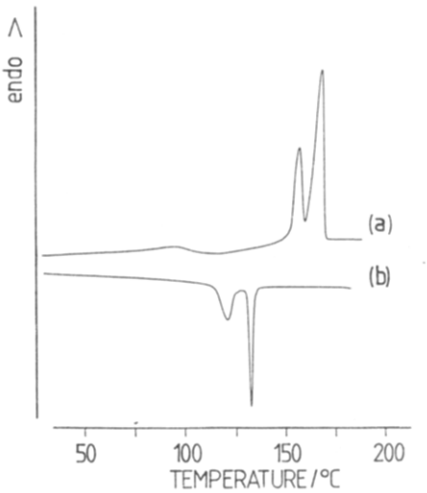

Figure 3. DSC traces for low molecular weight 2-4TDIBHHBP recorded at a 10 °C/min scanning rate: (a) heating; (b) cooling curves.

mately 142 and 138 °C are observed. The higher temperature exotherm, which (on the basis of optical microscopy) is associated with the isotropic–mesophase transition, is significantly narrower than its lower temperature counterpart, which is associated with the mesophase–crystal transition. The lower temperature transition is

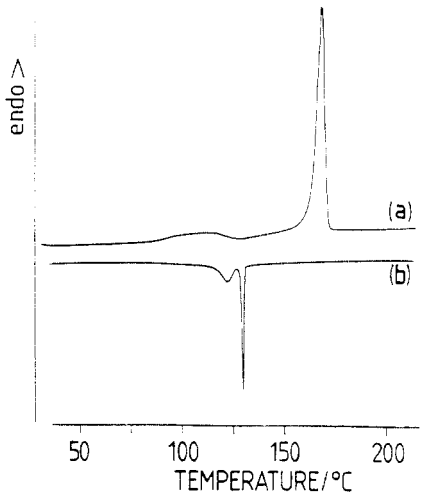

Figure 4. DSC traces for high molecular weight 2-4TDIBHHBP recorded at a 10 °C/min scanning rate: (a) heating; (b) cooling curves.

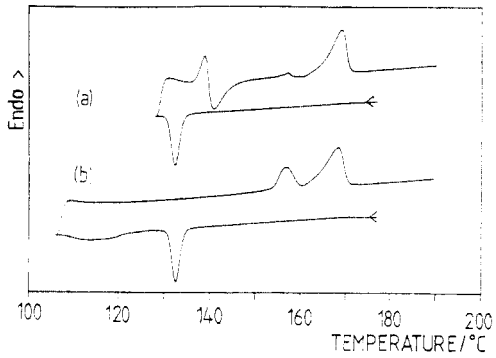

Figure 5. Cyclic cooling and heating scans for low molecular weight 2-4TDIBHHBP: (a) cooling through first exotherm only; (b) cooling through first and second exotherms. Scanning rate 10 °C/min.

skewed and extends to sufficiently low temperatures to obscure the features associated with the glass transition. The high molecular weight sample exhibits thermal behavior which is largely similar to that of the low molecular weight sample during 10 °C/min heating and cooling cycles (Figure 4), with the exception that only one endothermic peak is apparent on heating. The differences in thermal behavior as a function of molecular weight will be discussed below.

The effect of cooling a low molecular weight sample to a temperature which is just between the two regions of exothermic behavior observed in Figure 3 and immediate reheating is shown in Figure 5a. An endothermic peak is observed at approximately 135 °C at only slightly higher temperatures than the exothermic peak observed in the cooling half of the cycle. At still higher temperatures, further exothermic and endothermic behavior is observed which is attributed to crystallization and melting. Cooling through the second, a lower temperature exotherm in the cooling cycle (or annealing for more than a few minutes) leads to the DSC trace of Figure 5b which is similar to the trace from a sample scanned from ambient in which the onset of melting occurs at much higher temperatures, in the 158–170 °C region. This type of behavior is quite analogous to that observed in the optical microscope, where reversible isotropization of the threaded texture formed at 130 °C could be observed for samples which were annealed for less than 3–4 min and confirms that the isotropization temperature of the mesophase is lower than the crystalline melting point. Cooling a high molecular weight sample through its first

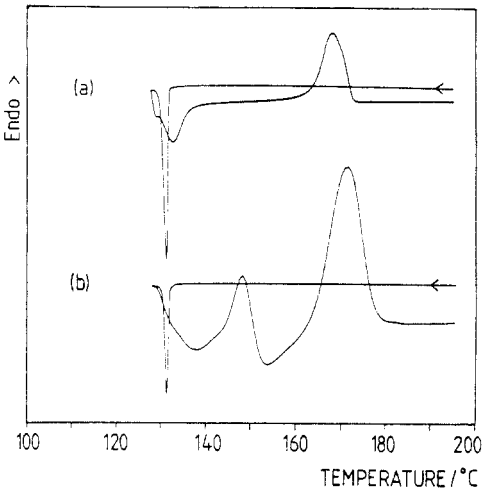

Figure 6. Cyclic cooling and heating DSC scans for high molecular weight 2-4TDIBHHBP: (a) 10 °C/min cooling and heating rates; (b) 10 and 100 °C/min cooling and heating rates, respectively.

cooling exotherm only and immediate reheating at 10 °C/min result in the DSC trace shown in Figure 6a. In this case, further exothermic behavior occurs on reheating the sample before isotropization can occur. If the temperature cycle with a 100 °C/min scanning rate in the heating cycle is repeated, the second exothermic process can be suppressed and the isotropization process observed, as can be seen in Figure 6b. The fact that a much faster heating rate is required to observe the isotropization of the mesophase in this sample relative to its low molecular weight counterpart indicates that crystallization of the mesophase occurs more rapidly for the high molecular weight polyurethane.

The qualitative observations outlined above regarding the kinetics of crystallization from the mesophase are reinforced by isothermal annealing studies performed specifically to study the crystallization processes occurring from the isotropic melt and from the mesophase. In the isotropic melt at 150 °C, where optical microscopy indicates that spherulitic growth is the only mechanism of crystal growth, it was found that the process was sufficiently slow to be followed by DSC. Samples were cooled from the isotropic melt at 220–150 °C and annealed for various times before being reheated at 10 °C/min in order to determine the melting enthalpy as a function of annealing time. Results for both high and low molecular weight samples are portrayed in Figure 7. It is readily apparent that the low molecular weight sample crystallizes more rapidly than its high molecular weight counterpart. Detailed fitting of the DSC data in Figure 7 to an Avrami equation requires a knowledg of the melting enthalpy of the 100% crystalline form (ΔH_∞) and of the density to estimate sample crystallinity.[22-25] Neither quantity is available for this polymer, and recognizing that the Avrami equation is simply an empirical means for the representation of crystal growth kinetics we have chosen to carry out the analysis using eq 1

$$\frac{\Delta H_\infty - \Delta H(t)}{\Delta H_\infty} = -\exp(-kt^n) \qquad (1)$$

where ΔH_∞ is the limiting value of the crystal melting enthalpy at long times. Using this value, we obtain a value for the Avrami exponent of $n = 2.6 \pm 0.2$, which is close to the value of 3 expected for three-dimensional crystal growth.

Crystallization from the mesophase, on the other hand, was found to occur much more rapidly. Crystallization

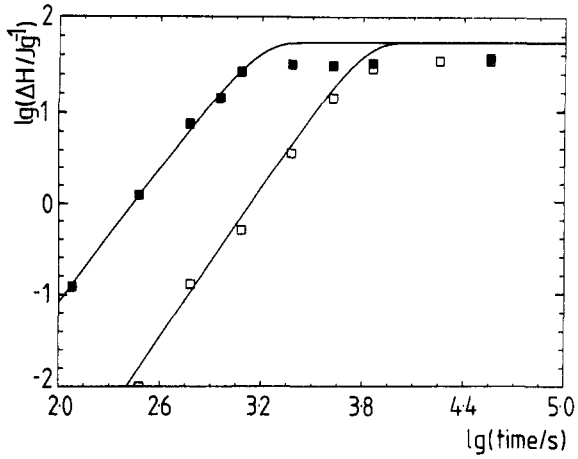

Figure 7. Melting entalphy vs annealing time data for low (□) and high (■) molecular weight 2-4TDIBHHBP. Crystallization temperature = 150 °C. Solid curves are fits to the Avrami equation using $\Delta H_0 = 54$ J g^{-1}. Fitting parameters: low molecular weight $n = 2.5 \pm 0.1$, $k^{-1/n} = 1900$ s; high molecular weight $n = 2.7 \pm 0.1$, $k^{-1/n} = 6400$ s.

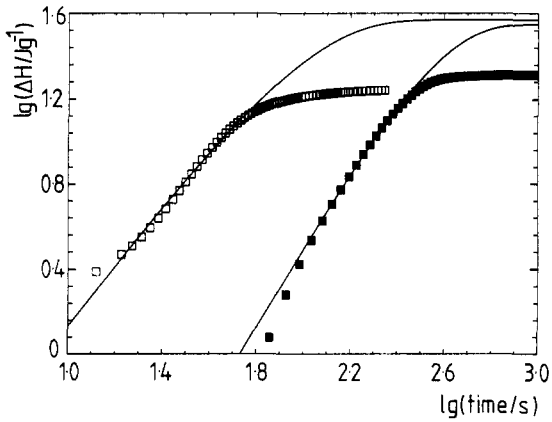

Figure 8. Melting entalphy vs annealing time data for low (□) and high (■) molecular weight 2-4TDIBHHBP. Crystallization temperature = 128 °C. Solid curves are fits to the Avrami equation. Fitting parameters: low molecular weight $n = 1.8 \pm 0.2$, $k^{-1/n} = 360$ s; high molecular weight $n = 1.4 \pm 0.2$, $k^{-1/n} = 100$ s.

kinetics in the mesophase were followed by cooling the sample through the isotropic–mesophase transition and annealing at 128 °C. At this temperature, the crystallization process was sufficiently rapid that the rate of heat evolution by the sample could be monitored directly by the DSC as a function of time. Upon integration, these data yield the total heat evolved (ΔH) during crystallization as a function of time and can be used to monitor the extent of crystallization. Data for both low and high molecular weight samples are shown in Figure 8. It is readily apparent that the low molecular weight sample crystallizes at a much slower rate than the high molecular weight sample, as was previously inferred from the behavior observd during cyclic temperature scans as discussed earlier in this paper. This contrasts with the behavior observed at 150 °C, where the low molecular weight sample crystallized most rapidly. The data obtained at 128 °C were also fitted to an Avrami analysis, with account being taken of the heat evolved on passing through the isotropic–mesophase transition. The theoretical fits obtained in this manner are also portrayed in Figure 9. The Avrami exponents thus estimated are $n = 1.8 \pm 0.2$ and $n = 1.4 \pm 0.2$ for low and high molecular weight samples, respectively. It may be noted that the fits to the Avrami equation are not as good at 128 °C as those obtained at 150 °C. In part, this reflects the presence of

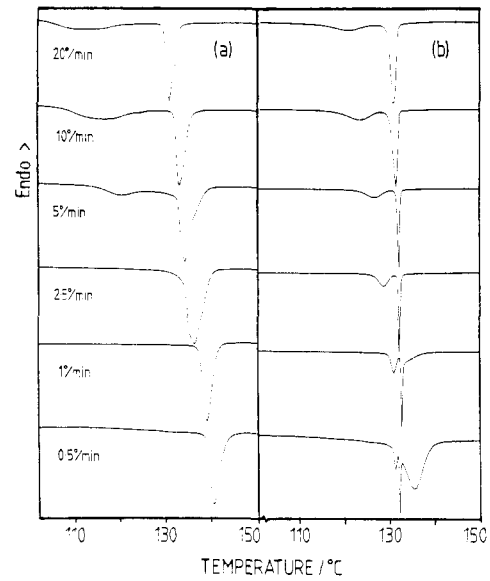

Figure 9. Cooling rate effects for (a) low and (b) high molecular weight 2-4TDIBHHBP.

short-time transient effects which occur when the DSC is switched from dynamic cooling to isothermal operation, which affect the DSC data and perhaps also the partial overlap of the isotropic–mesophase and mesophase–crystal transitions.

Overall crystallization kinetics were also studied qualitatively by using nonisothermal methods. The effect of cooling rate upon the nature of the exothermic processes that occur on cooling is illustrated in a and b of Figure 9 for high and low molecular weight samples, respectively. It is observed that as the scanning rate is reduced the lower temperature exotherm is shifted to higher temperatures and that for the low molecular weight sample the two-state exothermic process is replaced by a single-stage process at scanning rates slower than 2.5 °C/min. For the high molecular weight sample, which crystallizes at a slower rate from the isotropic melt, the two-stage ordering process observed at 10 °C/min cooling rate is never completely replaced by a single stage process. A new, higher temperature exotherm does, however, develop at scanning rates of 1 °C/min or slower—in a temperature range which is associated with spherulitic growth from the optical microscopic studies. Significantly, this peak is broader than the middle exotherm which is, on the basis of the optical microscopic evidence, to be associated with the appearance of the fluid-like threaded texture of the mesophase. This type of behavior strongly supports the notion that samples undergo an isotropic-to-liquid crystal transition when cooled from the melt at rates faster than 2.5 °C/min simply because the kinetics for crystallization from the isotropic melt are very slow. Once the mesophase is formed, crystallization occurs more rapidly from this partially ordered phase.

In order to elucidate further the thermal behavior of the polyurethane crystallized from the isotropic melt and from the mesophase, a series of low and high molecular weight samples were prepared by rapidly cooling from the isotropic melt at 220 °C to three different annealing temperatures, 150, 140, and 130 °C, where they were held for 8 h prior to being cooled to ambient. The series of samples thus subjected to a variety of annealing temperatures were then scanned at a variety of heating rates: 0.5, 10, and 100 °C/min. Results are displayed in a and b of Figure 10 for low and high molecular weight samples, respectively. Only data from 150 °C up are shown. Although other thermal events such as the glass transi-

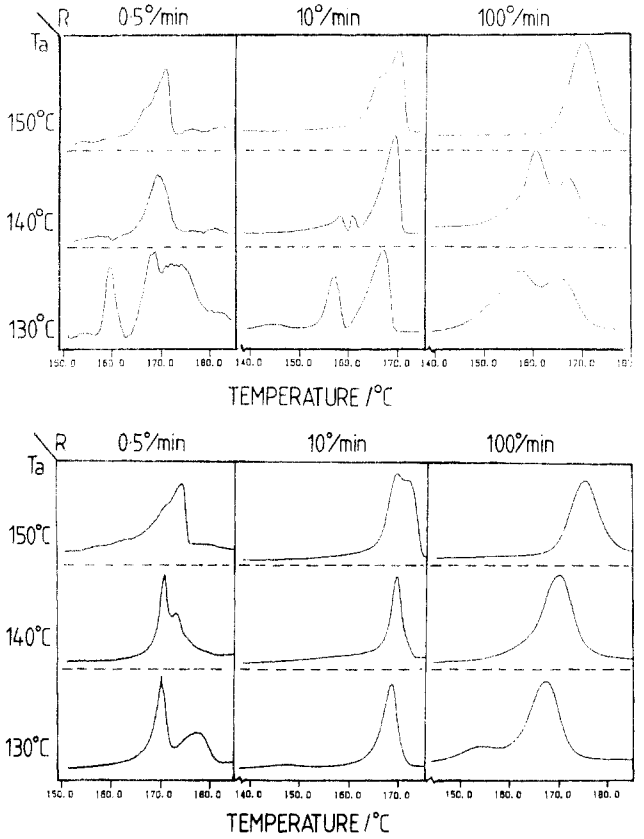

Figure 10. DSC heating traces for (a, top) low and (b, bottom) high molecular samples cooled from the melt to a variety of annealing temperatures (T_a) and then scanned at various heating rates (R).

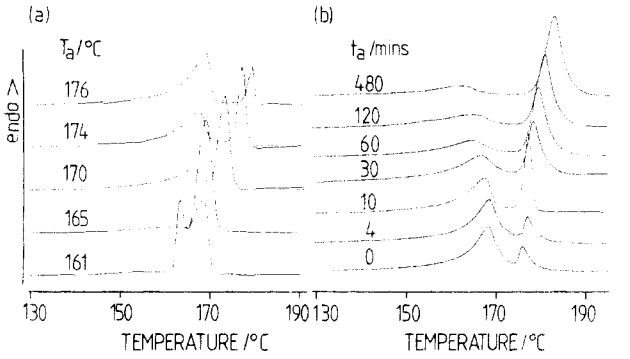

Figure 11. DSC traces recorded after 0.5 °C/min heating to (a) temperature T_a for 10 min and (b) to 174 °C and annealing for time t_a and then recooling. Low molecular weight 2-4TDIBHHBP.

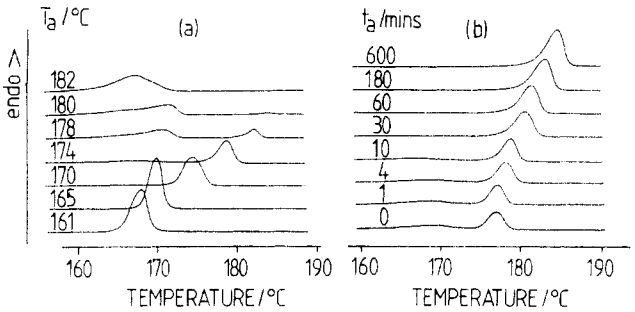

Figure 12. DSC traces recorded after 0.5 °C/min heating to (a) temperature T_a for 10 min and (b) to 174 °C and annealing for time t_a and then recooling. High molecular weight 2-4TDIBHHBP.

tion and "cold" crystallization occur between room temperature and 150 °C, they are not relevant to the present discussion. A number of differences between the thermal behavior of samples annealed at different temperatures are immediately apparent. Firstly, for the low molecular weight polymer only the sample annealed at 130 °C exhibits extension of the melting region and the formation of a new, high-temperature endothermic peak above 170 °C when scanned at 0.5 °C/min. In the case of the high molecular weight polymer, samples annealed at all three temperatures exhibit some extension of the melting region when scanned at 0.5 °C/min; however, this extension is much more pronounced in the case of the sample annealed at 130 °C; which is the only one to exhibit a new, clearly resolved, high-temperature peak. This type of behavior is not uncommon in semicrystalline polymers and is associated with the perfection, melting, and recrystallization of poorly formed crystals while heating.[26,28] Thus it appears that crystallization from the mesophase results in a crystal structure which is more amenable to perfection during slow heating than the spherulitic phase which forms from the isotropic melt. It is noted that at very slow heating rates (0.2 °C/min) the low-temperature peak at ca. 158 °C completely disappears and is replaced by a new high-temperature endotherm at ca. 180 °C while the peak at 170 °C remains largely unaffected. This suggests that the peak at 158 °C is to be associated with those crystals which are most amenable to perfection.

It is also apparent from Figure 10a that for the low molecular weight sample annealed at 140 °C a major shift of endothermic behavior from 170 to 160 °C occurs upon changing the scanning rate from 10 to 100 °C/min. This indicates that the crystalline material formed on annealing at 140 °C is initially in a low melting temperature form, which on heating at 10 °C/min reorganizes or melts and recrystallizes during the scan to a form which melts at 170 °C. At the faster scanning rate of 100 °C/min, the crystals do not have time to reorganize to this more stable form, and melting is observed at a lower temperature.

In order to study further the effect of annealing upon the high melting phase produced by slow heating of samples crystallized from the mesophase, samples of both low and high molecular weight polyurethanes were prepared by slowly heating samples through their normal melting zones and annealing for various times (t_a) and at various temperatures (T_a) before quenching back to room temperature and rescanning at 10 °C/min. DSC traces recorded for these series of thermal treatments are presented in Figures 11 and 12 for low and high molecular weight samples, respectively. It is observed that slow heating and annealing result in a peak—here termed the annealing peak—that has a melting temperature which is always above the annealing temperature and has an enthalpy which increases with annealing time. Endothermic peaks occurring below the annealing temperature result from the melting of material which is crystallized on cooling the annealed sample back to ambient prior to rescanning.

Peak positions (T_p) and enthalpies (ΔH) for the annealing peak, extracted from the traces in Figures 11 and 12, are plotted as a function of annealing temperature and annealing time in Figures 13 and 14, respectively. It is observed that there is a linear relationship between annealing temperature and peak position. At fixed annealing temperature, it is observed that peak enthalpy and temperature both increase with annealing time. Interestingly, in these slow heating and annealing experiments, the high molecular weight sample attains an initially greater level of crystallinity, as reflected by the larger fusion enthalpy of its annealing peak.

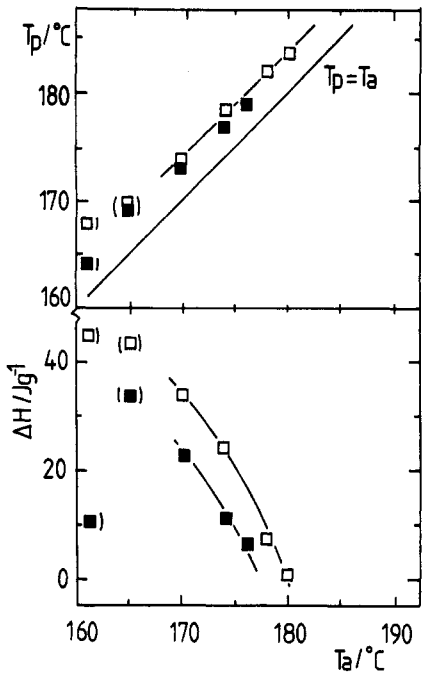

Figure 13. Peak position (T_p) and enthalpy (ΔH) as a function of annealing temperature (T_a) for the annealing peaks of Figures 11a and 12a. Low (□) and high (■) molecular weight 2-4TDIBHHBP.

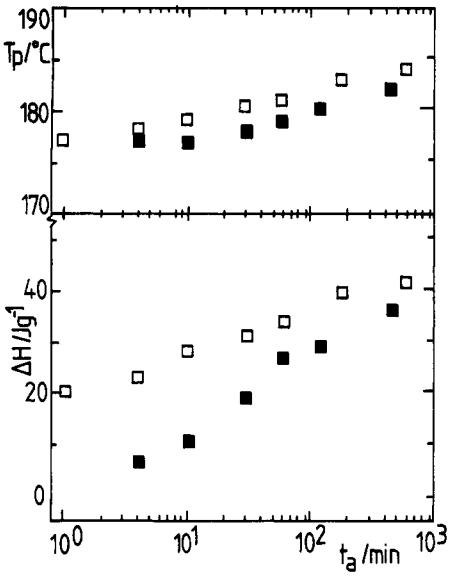

Figure 14. Peak position (T_p) and enthalpy (ΔH) as a function of annealing time (t_a) for the annealing peaks of Figures 11b and 12b. Low (□) and high (■) molecular weight 2-4TDIBHHBP.

Figure 15 compares the DSC trace of a low molecular weight sample, recorded after cooling from the isotropic melt to 174 °C and annealing for 8 h prior to cooling back to ambient and rescanning versus that of a sample heated from ambient to 174 °C at 10 °C/min and annealing for 8 h before cooling and rescanning. The trace from the sample annealed at 174 °C after cooling from the isotropic melt is the same as that of one cooled to ambient without annealing at 174 °C (see Figure 3, for example)—no endothermic behavior is observed above 170 °C. In contrast to this, the sample heated from ambient to 174 °C and annealed for 8 h prior to rescanning does show significant endothermic behavior above 174 °C. These observations combined with the behavior observed during the slow heating and annealing studies (Figures 12 and 13) indicate that the high-temperature melting phase observed on slow heating is produced by

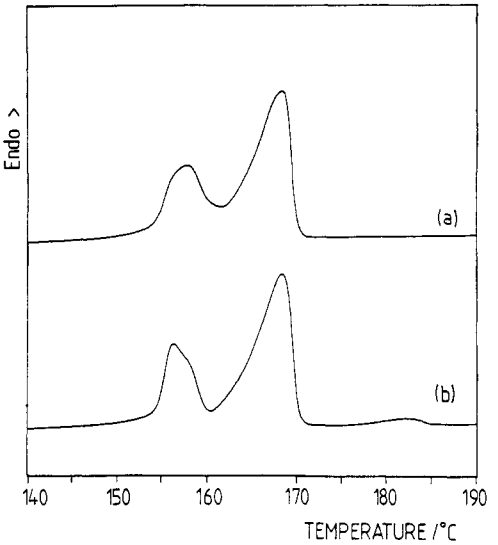

Figure 15. Comparison of annealing at 174 °C when 2-4TDIBHHBP is (a) cooling from melt or (b) heated from room temperature at 10 °C/min.

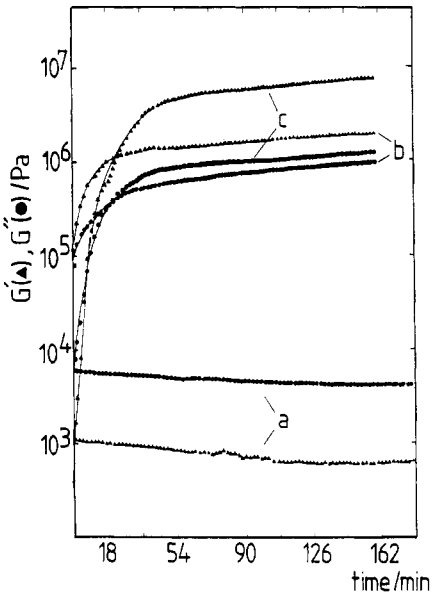

Figure 16. Dynamic rheology data for three different annealing histories (see text for details).

perfection of an already existing lower melting point phase which is formed when the sample is cooled back to ambient. The high melting point phase does not form from the isotropic melt.

These observations are reinforced by rheological investigations. Following the work of Lin and Winter,[30] the viscoelastic behavior of 24TDI/BHHBP subject to different thermal histories was studied. Figure 16 shows the evolution of the storage and loss moduli for three identically molded high molecular weight samples annealed for 150 min at 174 °C. Sample a was placed in the rheometer, melted at 210 °C, and carefully cooled at ca. 10 °C/min to 174 °C. Special care was taken to avoid undercooling in the sample due to the fluctuations in temperature that may occur during the transient behavior of the temperature controller. When the desired temperature was reached, measurements of G' and G'' were taken every 2 min for a period of 170 min. Liquid-like behavior with G'' higher than G' and low viscosity ($\eta^* = 4$ Pa s) was observed. The sample did not show any significant change in properties with time. The slight decrease in G' and G'' is attributed to sample loss, as part of it was slowly flowing out from between the plates.

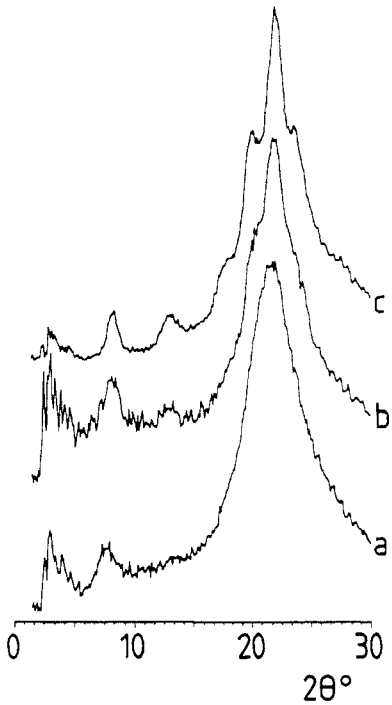

Figure 17. X-ray diffraction scans of the rheological samples (see text for details).

Sample b was placed in the rheometer and heated up to 160 °C. When the temperature of the sample reached equilibrium, the temperature was slowly increased at 2 °C/min up to 174 °C and then annealed under the same conditions as sample a. The initial storage modulus was now 2 orders of magnitude greater than in the previous case and increased rapidly during the first hour. The initial loss modulus, G'', was lower than G' and increased at a lower rate. The initial difference in behavior between these two samples is most likely due to the fact that sample b was not completely melted at the initial stage of the experiment. Visual observation of the sample showed that it remained opaque during the entire experiment. The changes in properties with time have been attributed to the melting and recrystallization of small, imperfect crystals into crystals with a higher degree of perfection.

Sample c was heated in the rheometer up to 184 °C and kept at that temperature for 2 min. At this stage, the polymer was transparent, as observed between the rheometer plates. The sample was then cooled to 174 °C at approximately 5 °C/min and annealed at that temperature. The initial behavior of the melt was the same as in sample a, but with this sample very rapid changes in properties were subsequently observed. The storage modulus G' increased by more than 3 orders of magnitude in the first hour, and G'' changed in the same period by about 1.5 orders. The magnitudes of G' and G'' at the end of the annealing were the highest for this set of experiments. In this case, the growth of high melting crystals in the sample is favored by the higher mobility of the melt and the presence of residual crystallites that are not completely melted at 184 °C. These crystallites act as nucleation sites.

These results parallel the changes observed Vectra with respect to the dynamic viscosity.[30] Additionally, X-ray diffraction results are also comparable. In Figure 17 are shown the 2θ versus intensity scans for samples a, b, and c for which the X-ray diffraction patterns are expected to exhibit not only the diffuse features associated with the vitrified mesophase glass formed on cooling back to ambient but also sharper features to be associated with any crystals which grow perfectly during the annealing process. Sample a shows only a broad reflection at approximately 22° and a weaker reflection at approximately 8°, ascribed to the smectic-like structure of the vitrified mesophase.[14] In sample b, some narrowing is observed as is the appearance of a shoulder at 20° and a small peak at 13°. Finally in sample c, where the greatest change in the complex modulus develops, many narrow reflections are observed, corresponding to the highest degree of order in the three samples. The spacing of the reflections observed in sample c is identical with those reported previously for annealed, oriented samples of this polymer as well as for unoriented samples crystallized from solution.[14]

The observations from the experiments outlined above allow a coherent interpretation of the temperature–phase behavior of these semirigid polyurethanes in terms of monotropic mesomorphic behavior. It is observed that crystallization can occur from either the isotropic melt or the mesophase and, in either case, results in the production of crystals which are stable above the mesophase–isotropic transition temperature. Moreover, there are a number of observable differences between the crystallization processes and thermal behavior of crystals produced from the isotropic melt and from the mesophase. First, the kinetics of crystallization are different. Crystallization from the isotropic melt is most rapid for the lower molecular weight sample, whereas crystallization from the mesophase is most rapid for the high molecular weight sample. Moreover, the Avrami exponents determined for crystallization of the isotropic melt are significantly smaller than those determined for the crystallization of the mesophase. Secondly, the optical textures of the crystalline phases produced from the isotropic melt and the mesophase differ greatly—crystallization from the isotropic melt results in a spherulitic morphology exhibiting negative birefringence whereas crystallization from the liquid mesophase preserves its threaded texture. Thirdly, and finally, crystals produced from the mesophase are much more readily perfected by slow heating and annealing than are crystals produced from the isotropic melt.

In order to arrive at a definitive explanation for the differences observed between samples crystallized from the mesophase and from the isotropic melt more, detailed morphological information than that which is available would be required. In the absence of such information, it is interesting to speculate about the reasons for the differences. The negative birefringence of spherulites grown from the isotropic melt indicates that the macromolecular chains in these spherulites are oriented to lie in the tangential direction, which suggests that the crystals have a chain folded character.[16] On the other hand, it has been proposed by Wendorff and co-workers[3,7] and by Blumstein et al.[31] that crystallization from the mesophase can preserve the local orientational order of the mesophase to produce chain-extended micellular type crystals. Such a crystallization process would account for the fact that the optical texture of the mesophase remains unchanged upon crystallization. It would also appear reasonable that chain-extended micellar crystals of the type proposed by Wendorff and co-workers[7] would be more amenable to perfection than would chain-folded crystals.

How differences in the molecular weight dependence of crystal growth rate for the two morphologies might arise is not so apparent. Generally, the effect of molecular weight upon crystallization rates is complex in poly-

meric materials.[32,33] A proper assessment can only be made at constant supercooling, not at constant temperature. The activation energy for diffusion, which is one of the factors determining the nucleation barrier height, is of crucial importance. In addition, effects such as the number density of chain end "defects" and orientational order parameter—which has been shown to increase with molecular weight—may prove important in determining the rate at which crystalline order propagates throughout the mesophase.[31]

The reduced values of the Avrami exponent, n, which are observed for crystallization from the mesophase as compared with the value observed for crystallization from the isotropic melt, are here interpreted as being indicative of the differences between the crystallization processes occurring in the two phases. The tendency toward parallel alignment of the polymeric chains, as noted previously, has a profound effect upon crystallization of the mesophase. Previous kinetic studies of the crystallization of mesomorphic polymers have been largely confined to the investigation of enantiotropic materials,[4,5,34-36] thus precluding comparison with the crystallization of the same material from the isotropic melt. In these previous studies, values of the Avrami exponent ranging from 0.8 to 4 have been reported. Yoo ahd Kim[35] in their investigations of semiflexible liquid crystalline polyesters have noted that the materials which undergo major textural changes under the optical microscope upon crystallization have larger Avrami exponents while those which exhibit little or no texture change have lower Avrami exponents. In the present study, the values of the Avrami exponent observed for mesophase crystallization fall in the lower range and are consistent with ordering in one or two dimensions as compared with the three-dimensional growth process associated with the larger exponent obtained for crystallization from the isotropic phase.

The fact that the low molecular weight sample normally exhibits two melting endotherms after annealing below the isotropic–mesophase boundary differentiates it from its high molecular weight counterpart. The slow heating studies indicate that the lower temperature peak is preferentially associated with the material which is most readily transformed into a higher melting temperature form. In view of the much faster crystallization kinetics observed for the low molecular weight sample in the isotropic melt as compared to the high molecular weight sample, it is speculated that the isotropic–mesophase boundary approached on cooling the low molecular weight material is also subject to some crystallization with chain folding, which results in mixed chain-extended and chain-folded morphologies. This in turn, it is speculated, leads to the double melting peak observed for low molecular weight samples annealed below the isotropic–mesophase boundary.

The fact that these polyurethanes can crystallize at all may, at first glance, seem surprising. It has been previously thought that the presence of the asymmetrically placed methyl group in the 24TDI unit suppresses the crystallization of such polymers.[37] Since previous studies of the crystallizability of 24TDI-based polyurethanes were limited to diols up to 12 carbons in length, it cannot be discounted that the ability of 24TDI/BHHBP to crystallize is due solely to its longer spacer length—equivalent to a 20–22-carbon diol.

On the other hand, for mesomorphic polymeric materials, there is evidence that disorder in the main chain is insufficient to suppress crystallization in some cases. As has been shown, in rigid rod polymers, the presence of random sequences is not sufficient to suppress crystallinity.[7,8] In addition to those systems having disorder in the sequence of the monomers along the chain, a number of polymers with regular repeat sequences but bearing bulky asymmetrically disposed side groups also exhibit a crystalline phase. The polyester based on terephthalic acid and 2-phenylhydroquinone has been shown to have significant three-dimensional order, inspite of the large asymmetrically placed phenyl group.[38] Bhattacharya and Lenz[39] have also noted that terpolymers of chlorohydroquinone, terephthalic acid, and hydroquinone exhibit a crystalline phase even though they contain both asymmetric chlorines and random comonomer sequences.

All the above-mentioned systems have considerably less conformational freedom available than is found in more or less flexible systems such as the one described in this work. Several such polymers which exhibit a mesophase have been shown to have a stable crystalline phase. Wendorff and co-workers[7] have noted crystallinity in copolyesters of the type

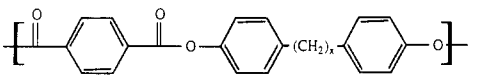

The systems examined had spacers of length 6 and 10 methylenes. Additionally, a system with a mixture of hexa- and decamethylene spacers gave crystalline reflections in the X-ray diffraction studies. It was noted that the crystalline structure indicated disordering of the spacer chains and positional ordering of the mesogenic units. Costa and co-workers[40] have reported crystallinity in copolyesters of the form

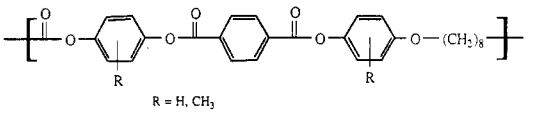

Again, the presence of random asymmetric methyl groups in the rigid unit does not seem to inhibit crystallization. In this study, however, little information was given as to the structure of the crystalline phase.

On the basis of the accumulated evidence from the studies outlined above, it would appear that the crystallization of these mesomorphic polymers in the presence of sequencing disorder is quite a widespread phenomenon and is not necessarily to be associated with the presence of long spacers. Turning once again to the discussion of the 24TDI/BHHBP polyurethanes, it would seem reasonable that the presence of rigid biphenyl units in the polymer main chain must enhance the tendency of these materials to crystallize and, by itself or in combination with the conformational flexibility of the methylene spacers, account for the development of crystallinity in these polyurethanes. The possibility of the mesogenic units causing an alignment of the chains and promoting crystallinity in such polymers has been examined by Flory, who envisaged the crystallization of these types of systems as a two-step process,[41] the first step involving the cooperative ordering of the chains into a parallel order, without any changes in intermolecular interactions, followed in a second step by an increase in the intermolecular interactions made possible by the more efficient packing of the chains in the parallel state. In the urethane system, the first step would involve development of mesomorphic order of preordering of chain segments in the isotropic melt due to the interaction of the biphenol units, with the hydrogen bonding between urethane units not developed to a high degree of order. Subsequently, the

urethane units become involved in more regular hydrogen bonding, helping to stabilize the three-dimensional structure.

One would presume that at temperatures where the hydrogen bonds were relatively stable they would tend to dominate the mobility of the system. Thus, at low temperatures, the formation of the initial ordered state mentioned above would be retarded, and the crystals formed would be imperfect. At higher temperatures, the rate of crystallization is dominated by stability of the crystalline nuclei, and without the presence of large crystalline nuclei such as are developed in the two-step annealing process, the rate of crystal growth is slow. Higher melting crystals developed from those formed at lower temperature are subject to perfection due to the labile nature of the hydrogen bonds and provide the nuclei for further crystal growth on annealing. As noted previously, it would appear that the crystals formed from the mesophase are most amenable to perfection.

Conclusions

(1) 24TDI/BHHBP exhibits monotropic mesomorphic behavior and exhibits two macroscopically distinct crystal morphologies—a spherulitic morphology produced from the isotropic melt and a threaded crystalline morphology when crystallized from the mesophase.

(2) Crystals produced from the isotropic melt and from the mesophase differ from each other with respect to the molecular weight dependence of the crystallization kinetics and in the ability to produce high melting point phases on annealing or slow heating. Inasmuch as the Avrami exponents for crystallization from the isotropic melt and from the mesophase differ significantly, it appears that the mechanism of crystallization from these two phases is also different.

(3) The development of the ordered crystalline phase depends on the presence of preformed nuclei, developed at lower temperatures in the mesophase.

Acknowledgment. We thank Drs. S. W. Kantor and H. H. Winter for useful discussions and Dr. F. E. Karasz for use of his X-ray diffraction facility. We also acknowledge financial support from the Army Research Office, Grant ARO-23941-CH (W.J.M. and S.L.H.), and a grant from the National Science Foundation, Polymers Program, Grant No. DMR 8919-105 (S.L.H.).

References and Notes

(1) Permanent address: (a) ICI Chemicals & Polymers, The Heath, Runcorn, Cheshire WA7 4QD, England. (b) PLAPIQUI, C. C. 717, Bahia Blanca, 8000 Argentina. (c) Department of Materials Science and Engineering, University of Cincinnati, 498 Rhodes Hall, Cincinnati OH 45221-0012. (d) Shell Development Co., Westhollow Research Center, P.O. Box 1380, Houston, TX 77001.
(2) Butzbach, G. D.; Wendorff, J. H.; Zimmermann, H. J. *Polymer* **1986**, *27*, 1337.
(3) Bechtoldt, H.; Wendorff, J. H.; Zimmerman, H. J. *Makromol. Chem.* **1987**, *188*, 651.
(4) Grebowicz, J.; Wunderlich, B. *J. Polym. Sci., Polym. Phys. Ed.* **1983**, *21*, 141.
(5) Cheng, S. Z. D. *Macromolecules* **1988**, *21*, 2475.
(6) Lemmon, T. J.; Hanna, S.; Windle, A. H. *Polym. Commun.* **1989**, *30*, 2.
(7) Wendorff, J. H.; Frick, G.; Zimmerman, H. *Mol. Cryst. Liq. Cryst.* **1988**, *157*, 455.
(8) Biswas, A.; Blackwell, J. *Macromolecules* **1988**, *21*, 3146, 3152, 3158.
(9) Gutierrez, G. A.; Chivers, R. A.; Blackwell, J.; Stamatoff, J. B.; Yoon, H. *Polymer.* **1983**, *24*, 937.
(10) Blackwell, J.; Gutierrez, G. A.; Chivers, R. A. *Macromolecules* **1984**, *17*, 1219.
(11) Chivers, R. A.; Blackwell, J.; Gutierrez, G. A. *Polymer* **1984**, *25*, 435.
(12) Windle, A. H.; Viney, C.; Golombok, R.; Donald, A. M.; Mitchell, G. R. *Faraday Discuss., Chem. Soc.* **1985**, *79*, 55.
(13) Stenhouse, P. J.; Vallés, E. M.; MacKnight, W. J.; Kantor, S. W. *Macromolecules* **1989**, *22*, 1467.
(14) Pollack, S. K.; Shen, D. Y.; Wang, Q.; Stidham, H. D.; Hsu, S. L. *Macromolecules* **1989**, *22*, 551.
(15) Smyth, G.; Grebowicz, J.; Stenhouse, P. J.; MacKnight, W. J.; Kantor, S. W. *Proceedings of the Seventeenth North American Thermal Analysis Society Conference*; Earnest, C. M., Ed.; October 1988, Vol. II, p 424.
(16) Bassett, D. C. *Principles of Polymer Morphology*; Cambridge University Press: Cambridge, 1981.
(17) Hemsley, D. A. *The Light Microscopy of Synthetic Polymers*; Oxford University Press: New York, 1984.
(18) Demus, D.; Richter, L. *Textures of Liquid Crystals*; Verlag Chemie: Weihheim, 1978.
(19) Nöel, C. In *Recent Advances in Liquid Crystalline Polymers*; Chapoy, L. L., Ed.; Elsevier Applied Science Publishers: New York, 1985.
(20) Barrall, E. M. In *Liquid Crystals: The Fourth State of Matter*; Saeva, F. D., Ed.; Marcel Dekker: New York, 1979.
(21) Zhou, Q. F.; Duan, X. L.; Liu, Y. L. *Macromolecules* **1986**, *19*, 247.
(22) Wunderlich, B. *Macromolecular Physics*; Academic Press: New York, 1973, 1976; Vols. 1, 2.
(23) Mandelkern, L. *Crystallization in Polymers*; McGraw-Hill: New York, 1964.
(24) Avrami, M. J. *J. Chem. Phys.* **1939**, *7*, 1103; **1941**, *8*, 212; **1941**, *9*, 177.
(25) Cheng, S. Z. D.; Wunderlich, B. *Macromolecules* **1988**, *21*, 3327.
(26) Wunderlich, B. *Macromolecular Physics*; Academic Press: New York, 1980; Vol. 3.
(27) Pollack, S. K.; Smyth, G.; Hsu, S. L.; MacKnight, W. J. *Macromolecules*, submitted for publication.
(28) Holdsworth, P. J.; Turner-Jones, A. *Polymer* **1971**, *12*, 195.
(29) Hoffman, J. D.; Weeks, J. J. *J. Res. Natl. Bur. Stand.* **1962**, *66A*, 13.
(30) Lin, Y. G.; Winter, H. H. *Macromolecules* **1988**, *21*, 2439.
(31) Biumstein, R. B.; Stickles, E. M.; Gauthier, M.; Blumstein, A.; Volino, F. *Macromolecules* **1984**, *17*, 177.
(32) Fatou, J. G. *Makromol. Chem. Suppl.* **1984**, *7*, 131.
(33) Magill, J. H. *Polym. Lett.* **1968**, *6*, 853.
(34) Warner, S. B.; Jaffe, M. *J. Cryst. Growth* **1980**, *48*, 184.
(35) Yoo, Y. D.; Kim, S. C. *Polym. J.* **1988**, *20*, 1117.
(36) Liu, X.; Hu, S.; Shi, L.; Xu, M.; Zhou, Q.; Duan, X. *Polymer* **1989**, *30*, 273.
(37) Brunette, C. M.; Hsu, S. L.; MacKnight, W. J. *Macromolecules* **1982**, *15*, 71.
(38) Hong, S. K.; Blackwell, J. *Polymer* **1989**, *30*, 225.
(39) Bhattacharya, S. K.; Lenz, R. W., submitted for publication.
(40) Costa, G.; Nora, A.; Trefiletti, V.; Valenti, B. *Mol. Cryst. Liq. Cryst.* **1988**, *157*, 79.
(41) Flory, P. J. *Proc. R. Soc. (London)* **1956**, *A234*, 60.